Chapter III. Dynamic properties of artificial protein hydrogels assembled through aggregation of leucine zipper peptide domains

Abstract

Network relaxation behavior of genetically engineered multidomain protein ($AC_{10}A$) hydrogels was investigated by rheological methods including oscillatory shear and creep measurements. The longest stress relaxation time of these physical gels exhibited a strong dependence on pH, varying from ca. 70 seconds at pH 8.0 to ca. 1000 seconds at pH 7.0. The pH-responsiveness of material properties is regulated by the electrostatic interactions among the residues on the *e* and *g* positions of the leucine zipper domain. The kinetics of strand exchange of the associative leucine zipper domains was studied by a method based on fluorescence self-quenching and dequenching. A fluorescein-labeled leucine zipper solution, in which fluorescence was quenched because fluorophores were brought into proximity by self-assembling leucine zipper strands, was mixed with an unlabeled leucine zipper solution in a volumetric ratio of 1:60. The time course of the increase in fluorescence emission intensity following the mixing revealed the characteristic strand exchange time of the leucine zipper domain. This characteristic time changed with pH from ca. 200 seconds at pH 8.0 to ca. 4500 seconds at pH 7.0. The longest stress relaxation time of $AC_{10}A$ hydrogels and the strand exchange time of the leucine zipper A are on the same order of magnitude at each pH value and vary with pH in parallel. This correlation supports the key assumption in transient network theories: network relaxation is limited by the lifetime of associative groups in transient junctions.

It also provides insights into molecular design strategies to tune network relaxation behavior and related material properties of artificial protein hydrogels.

1. Introduction

$AC_{10}A$ hydrogels are transient networks formed through physical interactions, which are temporal in the sense that they can break and reform on a certain time scale. These networks are analogous to chemically crosslinked networks on short time scales, as indicated by a plateau storage modulus in high frequency regime of oscillatory deformation; but they are liquid-like on long time scales. Dynamics of these networks is as critical as structure in determining material properties.

Although storage modulus (determined by the structure of a network) is important when materials are used in applications such as tissue engineering scaffolds, other physical properties may become primary design parameters for different applications. For example, when hydrogels are used to immobilize cells or macromolecular drugs, the ability to trigger a sharp transition in viscosity is valuable. The theory of linear viscoelasticity suggests that the zero-shear viscosity, defined by the viscosity at vanishing shear rate ($\dot{\gamma} \to 0$), is determined by both the plateau storage modulus and the longest stress relaxation time[1]:

$$\eta(\dot{\gamma} \to 0) = G'_{\infty}\tau_r \qquad (1)$$

where η is viscosity, G'_{∞} is the plateau storage modulus, and τ_r is the longest stress relaxation time. To control the viscosity of these materials, understanding their dynamic properties and the underlying molecular basis is as important as understanding their structural properties.

Such studies are also important from fundamental perspectives. Transient-network theories[2-5], which derive from the theory of relaxing polymeric media originally proposed by Green and Tobolsky[2], argue that the stress relaxation time of a transient network is regulated by the lifetime of the associative group in the physically assembled junctions. However, few efforts have been made to experimentally test this argument on a molecular level[6] and the subject remains controversial[7]. NMR studies revealed the exchange characteristic time for a C_{12} hydrophobe attached on poly(sodium acrylate) to be 14 ms at 25 °C[6]. However, Annable reported that transient networks formed from HEUR (hydrophobically modified urethane-ethoxylate) polymers with C_{12} and C_{20} hydrophobes had a single stress relaxation time of ca. 1 ms and 6 s, respectively, at 25 °C[3]. Ng et al. argued that the rheological data of transient networks formed from HEUR polymers should be fit with a two-mode Maxwell model. They showed that networks formed from HEUR polymers with C_{20} hydrophobes have two stress relaxation times: one is ca. 6 s and the other is in the range of 0.01-0.1 s. They suggested that the lifetime of hydrophobes is directly related to the fast mode of material stress relaxation.

In the present artificial protein hydrogels, therefore, we independently determined the network stress relaxation time and the leucine zipper strand exchange time to examine their relationships. Network relaxation behavior of $AC_{10}A$ hydrogels was studied using rheological measurements. The strand exchange time of the associative leucine zipper domain was probed using a fluorescence method. The correlation between the macroscopic dynamic behavior of $AC_{10}A$ hydrogels and the strand exchange kinetics of the leucine zipper domain A was evaluated. The molecular origin of the material properties' pH-responsiveness was also examined.

2. Experimental section

2.1. Protein synthesis and purification

Amino acid sequences of the proteins to be discussed in this chapter are shown in Scheme 1. Expression vectors pQE9AC$_{10}$Atrp, pQE9Acys, and pQE9Atrp were constructed previously by Petka[8].

An oligonucleotide segment (T) encoding the thrombin cleavage site (LVPRGS) was excised from pUC18L2T[9] by digestion with *Nhe*I and *Spe*I, and ligated into the *Nhe*I site of pUC18L2A[8] and pUC18L1A[8], respectively. The DNA segments encoding TAcys and TAtrp were excised from the resulting pUC18L2TA and pUC18L1TA, respectively, by digestion with *Bam*HI and inserted into the *Bam*HI site of the pQE9 vector to yield pQE9TAcys and pQE9TAtrp. The sequences were verified at the DNA sequencing core facility of the Beckman Institute at the California Institute of Technology.

The newly constructed expression vectors were each transformed into *Escherichia coli* strain SG13009, which carries the repressor plasmid pREP4 (Qiagen, Chatsworth, CA). Proteins AC$_{10}$Atrp (AC$_{10}$A), Acys, Atrp, TAcys, and TAtrp were expressed as described in Chapter II and purified by affinity chromatography on a nickel nitrilotriacetic acid resin (Qiagen, Chatsworth, CA) through a 6×histidine tag encoded in the pQE9 vectors.

2.2. Enzymatic cleavage of the N-terminal histidine tag

Solutions of TAtrp and TAcys (100 μM) were prepared in thrombin cleavage buffer (50 mM Tris·Cl, 150 mM NaCl, 2.5 mM $CaCl_2$, pH 7.5). A 0.5 unit/μL thrombin (from human plasma, Sigma-Aldrich, St. Louis, MO) stock solution was prepared and

added to the TAtrp and TAcys solutions, respectively, to a final concentration of 0.002 units/μL. Each sample was incubated at room temperature for 4 hours, and loaded on a column packed with nickel nitrilotriacetic acid resin (Qiagen, Chatsworth, CA), followed by washing with twice the resin volume of 8 M urea (pH 8.0). The flow-through was collected, dialyzed against sterile deionized water, and lyophilized. Matrix-assisted laser desorption ionization mass spectrometry (MALDI-MS) conducted with a 10 mg/mL sinapinic acid matrix solution on a Voyager mass spectrometer (Applied Biosystems) revealed a single peak with a mass shift of 2617 Da and 2802 Da, respectively, from that of the intact TAtrp and TAcys, suggesting that the segment upstream to the thrombin cleavage site (expected to be 2628 Da and 2815 Da, respectively) was completely cleaved.

2.3. Fluorescent labeling

Fluorescein maleimide was site-specifically ligated to the cysteine residue engineered at the C-termini of Acys and TAcys (histidine tag cleaved, no-6H-TAcys), respectively. Protein solutions were prepared in phosphate buffer (10 mM NaH_2PO_4, 90 mM NaCl) at a concentration of 100 μM. A tris(2-carboxyethyl)phosphine hydrochloride (TCEP) (Pierce, Rockford, IL) stock solution (100 mM) was added into each protein solution to a final concentration of 2 mM. The pH of the mixture was adjusted to 4.5, followed by incubation at room temperature for half an hour to allow reduction of disulfide bonds. The pH was then adjusted to 5.5. A fluorescein-5-maleimide (Molecular Probes, Eugene, OR) stock solution (100 mM) was freshly prepared in DMSO, and added

into each reduced protein solution to a final concentration of 1 mM. The mixture was incubated in the dark at room temperature for half an hour.

The sample was concentrated from 10 mL to 1 mL with Centricon YM-3 centrifugal filter unit (molecular weight cutoff 3000, Millipore, Billerica, MA), followed by gel filtration on a Sephadex G-25 (Amersham Biosciences, Piscataway, NJ) column (1.5 cm diameter × 30 cm height) to remove unreacted dye. The protein fraction was collected, dialyzed against sterile deionized water, and lyophilized in the dark.

The absorbance at 515 nm measured on a Cary 50 Bio UV-vis spectrophotometer (Varian, Palo Alto, CA) showed that in different batches of labeling reaction 20-40% of Acys was labeled on the basis of an extinction coefficient of 83000 M^{-1} cm^{-1} for fluorescein maleimide.

2.4. Rheological measurements

$AC_{10}A$ solutions were prepared in phosphate buffer (13 mM $NaH_2PO_4 \cdot H_2O$, 87 mM $Na_2HPO_4 \cdot 7H_2O$) with the pH value adjusted as needed. Each solution was centrifuged to remove entrapped bubbles and then loaded on rheometers. Frequency sweep measurements were carried out under a 1% strain on an RFS III rheometer (TA Instruments, New Castle, Delaware) with a cone-and-plate geometry (0.04 rad cone angle and 25 mm diameter). The edge of each sample was covered with mineral oil to minimize solvent evaporation. Creep tests were conducted under a 100 Pa stress on a SR-5000 stress rheometer (Rheometric Scientific, Piscataway, NJ) equipped with a solvent trap. A cone-and-plate geometry (0.1 rad cone angle and 25-mm diameter) was used. The

temperature was controlled at 22.0 ± 0.1 °C by a Peltier thermoelectric device for each measurement.

2.5. Strand exchange experiments

Solutions of labeled leucine zipper (Acys-FM or no-6H-TAcys-FM) and unlabeled leucine zipper (Atrp or no-6H-TAtrp) were prepared in phosphate buffer (13 mM $NaH_2PO_4 \cdot H_2O$, 87 mM $Na_2HPO_4 \cdot 7H_2O$) at a concentration of 100 μM. The unlabeled protein solution (2 mL) was placed in a cuvette and stirred by a magnetic stirring bar at the maximum speed in the sample compartment of a fluorometer (Photon Technology International, Inc., Lawrenceville, NJ). The labeled solution (35 μL) was injected rapidly into the unlabeled solution. The sample was excited at 495 nm, and emission at 515 nm was monitored as a function of time for 2 hours after the injection at an acquisition rate of 25 data points per second. The temperature was controlled at 22 °C.

The time course of fluorescence de-quenching was analyzed with non-linear exponential decay fitting using Origin 6.1 software (OriginLab Corporation, Northampton, MA).

3. Results and discussion

3.1. Network relaxation behavior of $AC_{10}A$ hydrogels

As discussed in Chapter II, the linear viscoelastic behavior of $AC_{10}A$ networks was characterized using oscillatory frequency sweep measurements. The dynamic moduli show a prominent loss peak (maximum in the loss modulus G″) that coincides with the frequency ω_x at which G′ and G″ cross (Figure 3.1 (a)). The crossover coincides with a

45° phase angle between oscillatory stress and applied strain (Figure 3.1 (b)). Loss peaks indicate energy-dissipating molecular motions at the corresponding time scales (stress relaxation times). At pH 8.0, the dominant loss peak separates a high frequency elastic plateau and low frequency regime in which $G' \sim \omega^{1.7}$ and $G'' \sim \omega^{0.9}$. These exponents approach the expected values in the terminal regime (2 and 1)[10], so the characteristic frequency of the dominant loss peak corresponds to the longest stress relaxation time of the network ($\tau_r \sim 1/\omega_x$). τ_r dominates the relaxation behavior of $AC_{10}A$ networks and controls their viscosity, and hence is the focus of this study. As shown in Figure 3.1, τ_r of $AC_{10}A$ transient networks varies from ca. 100 seconds at pH 8.0 to ca.1000 seconds at pH 7.0. These time scales are much longer than those of transient networks assembled through aggregation of hydrophobic chemical groups. For example, the typical τ_r of a network formed from a hydrophobically modified urethane-ethoxylate (HEUR) polymer is on the order of 0.001-1 second[3].

However, oscillatory frequency sweep measurements are not suitable for quantitative determination of τ_r. Due to the limited frequency range of the instrument, only half of the dominant loss peak can be acquired at pH 7.0. (Because the secondary structure of the leucine zipper A becomes denatured at elevated temperatures, temperature-frequency superposition cannot be applied.) Each frequency sweep takes ca. 10 hrs to cover the five decades from 100 rad/s to 0.001 rad/s at 5 data points/decade. During this time, solvent evaporation was inevitable even though the sample was covered by mineral oil. Therefore, creep tests were exploited to quantitatively determine the longest stress relaxation time of $AC_{10}A$ hydrogels.

In each creep test, a constant stress of 100 Pa was applied and the strain was recorded as a function of time until a steady state of straining was reached. A steady state of straining is indicated when the strain recovery upon removal of the stress equals the strain intercept of the creep curve extrapolated to zero time using the slope of the last several points before removing the stress[11] (Figure 3.2(a)). The longest stress relaxation time is calculated as follows[11]:

$$\tau_r = \gamma_e^{\,0} / \dot{\gamma}_\infty \qquad (2)$$

Where $\gamma_e^{\,0}$ is the strain intercept of the extrapolated steady state creep curve at t=0 and $\dot{\gamma}_\infty$ is the steady rate of straining.

A pronounced decrease in the steady rate of straining $\dot{\gamma}_\infty$ was observed when pH was decreased from 8.0 to 7.0, while $\gamma_e^{\,0}$ did not change significantly (Figure 3.2 (b)). τ_r varies from ca. 80 seconds at pH 8.0 to ca. 950 seconds at pH 7.0, as calculated on the basis of Equation (2).

3.2. Strand exchange kinetics of the leucine zipper domain

The kinetics of strand exchange of the associative leucine zipper was studied by a method based on fluorescence self-quenching and dequenching[12]. Proteins containing only the leucine zipper domain A were used, some labeled with fluorescein (Acys-FM) and some unlabelled (Atrp). A solution containing Acys-FM (the extent of labeling is ca. 20-40%) was mixed with a solution containing only unlabeled leucine zippers (Atrp) in a volumetric ratio of 1:60. The time course of the increase in fluorescence emission intensity following the mixing revealed the characteristic time of leucine zipper strand

exchange. Control experiments under denaturing conditions were used to identify the characteristic time associated with leucine zipper strand exchange.

The time course of the fluorescence emission in a strand exchange experiment for 100 μM, pH 7.4 leucine zipper solutions in phosphate buffer is shown in Figure 3.3. Fluorescence dequenching under these conditions involves two clearly de-coupled phases. A fit to a double exponential relaxation process reveals a characteristic time of 17.7 ± 0.2 seconds for the fast phase and a characteristic time of 950.9 ± 0.5 seconds for the slow phase.

Control experiments under denaturing conditions (in 8 M urea, pH 7.4) were carried out and the time course of the fluorescence emission is shown in Figure 3.3. The slow phase of the increase in fluorescence disappeared in these control experiments, suggesting that it was intrinsic to leucine zipper strand exchange under native conditions. The transient response of the fluorescence signals under denaturing conditions exhibits a single exponential relaxation with a characteristic time of 15.8 ± 0.1 seconds (Figure 3.3). Since denatured leucine zippers do not bring fluorophores into proximity, most likely fluorescence was quenched through non-specific association of fluorophores and dequenched when the labeled species were diluted. (Fluorescein is itself hydrophobic and has some tendency to associate in aqueous media.) The consistency between the characteristic time of the fast phase in strand exchange experiments and that in denatured control experiments suggests that the fast phase is not intrinsic to leucine zipper strand exchange. Since the extent of labeling is only ca. 20-40%, and leucine zipper strands can adopt antiparallel orientation in aggregates, even under native conditions not every fluorophore is brought into proximity of another fluorophore through leucine zipper

aggregation. Nevertheless, the fluorescence of these fluorphores may be quenched by non-specific association driven by fluorescein. This component of quenching is dequenched upon mixing on a time scale much faster than strand exchange.

The slow relaxation in strand exchange experiments depends strongly on pH (Figure 3.4). The characteristic times obtained from data fitting to a double exponential relaxation processes (Table 1) show that leucine zipper strand exchange time τ_2 changes from ca. 200 seconds at pH 8.0 to ca. 4500 seconds at pH 7.0. In contrast, τ_1 shows no obvious change and remains between 10 and 20 seconds at all pH values examined, consistent with the characteristic time revealed from control experiments under denaturing conditions. Each experiment was repeated 2-3 times using Acys-FM from different batches of labeling reaction. The revealed strand exchange time is consistent under each condition.

Strand exchange experiments for solutions at concentrations of 50 μM and 200 μM (pH 7.4) showed no obvious concentration dependence of the leucine zipper strand exchange time τ_2, suggesting that leucine zipper strand exchange is a first-order process (most likely the dissociation process).

3.3. Relating relaxation behavior of $AC_{10}A$ networks to the molecular dynamic properties of the leucine zipper domain

A comparison of the relaxation behavior of $AC_{10}A$ hydrogels and the strand exchange kinetics of the associative leucine zipper domain reveals a strong correlation between macroscopic and molecular dynamic properties (Figure 3.5). The longest stress relaxation time of $AC_{10}A$ hydrogels and the strand exchange time of the leucine zipper

domain A are on the same order of magnitude at each pH value, and vary with pH in parallel. From a fundamental perspective, this correlation provides direct experimental evidence for the argument made in transient network theories: network relaxation is limited by the lifetime of associative groups in transient junctions. From the material design point of view, this result suggests that network relaxation behavior and the related material properties, such as viscosity, of these artificial protein hydrogels can be tuned by controlling leucine zipper strand exchange kinetics.

At each pH value, the strand exchange time of the leucine zipper domain is ~3-4 times greater than the stress relaxation time of an $AC_{10}A$ hydrogel. This discrepancy is consistent with the strong tendency of $AC_{10}A$ to form looped rather than bridged configurations in networks. The transient network theory developed by Annable[3] suggests that superbridges (as shown in Figure 3.6 (b)) accelerate the stress relaxation time of the network due to the increase in probability of breaking the bridges that sustain stresses. Annable proposed that the relationship between the stress relaxation time of a transient network (τ_r) and the relaxation time of a single-chain bridge (τ_a) was as follows,

$$\tau_r/\tau_a=P(>2)/P(>1) \qquad (3)$$

where P(>2) was the number of the aggregates having functionalities larger than 2, and P(>1) was the number of the aggregates having functionalities larger than 1. In an $AC_{10}A$ transient network, there are three possible states for tetrameric leucine zipper aggregates (Figure 3.6 (a)). P(>2) is the number of the aggregates in state A, and P(>1) is the number of the aggregates in states A and B. As will be discussed in Chapter IV, there are 2-3 times as many aggregates in state B as in state A, on the basis of rheological data and a model. Therefore, the present experimental observations are quite consistent with

Annable's theory, and suggest that the lifetime of associative groups is directly responsible for the relaxation time for the stresses sustained by single-chain bridges.

3.4. Molecular basis underlying the pH-responsiveness of dynamic properties

One of the particular advantages of artificial proteins as responsive hydrogels is the ability to precisely control the conditions at which transitions in material properties, such as viscosity, occur. Petka[8] showed that $AC_{10}A$ solutions exhibit a sharp transition in viscosity (90% of the change in viscosity occurs over 1 pH unit between 7 and 8). The present study showed a ten-fold increase in network stress relaxation time, and hence the zero-shear viscosity, over the same pH range. Furthermore, the transition pH can be tuned by choice of amino acid residues.

Regarding leucine zipper strand exchange kinetics and relaxation behavior of $AC_{10}A$ networks, two conjectures were made to explain why the transition occurs near neutral pH. One explanation focused on the repulsive interactions among negatively charged glutamic acid residues in the leucine zipper upon deprotonation at high pH. Because the observed transition pH is much greater than the pKa of glutamic acid (4.4), an alternative explanation focused on the histidine residues (engineered at the N-terminus of each protein for purification purpose), which have a pKa of 6.5. In both scenarios the material has faster stress relaxation (lower viscosity) at high pH. In the first scenario, electrostatic repulsion at high pH destabilizes leucine zipper aggregation and accelerates their strand exchange. The transition pH is controlled by the pKa of glutamic acid residues, which can be shifted to pH ~7-8 by proximate hydrophobic residues[13]. In the second scenario, the histidine tag gradually becomes positively charged as pH decreases

near neutral pH, interacting with negatively charged glutamic acid resiudues in the leucine zipper and slowing down the strand exchange kinetics.

To test the second conjecture, a thrombin cleavage site was genetically engineered between the histidine tag and the leucine zipper domain (TAcys and TAtrp). After purification of the proteins, the histidine tag was enzymatically cleaved (no-6H-TAcys and no-6H-TAtrp). The strand exchange times (the slow times) revealed from double exponential fits to the time courses of fluorescence increase in the strand exchange experiments (at pH 7.4) are 950.9 ± 5.1 seconds (for Acys-FM + Atrp) and 955.6 ± 13.0 seconds for (no-6H-TAcys-FM + no-6H-TAtrp). The similarity between these two strand exchange times is clearly evident in the parallel time courses on a semi-log plot (inset, Figure 3.7). The difference in the amplitude of the fluorescence dequenched through strand exchange is probably due to different extents of labeling. This result suggests that the histidine tag does not play a role in controlling the kinetics of leucine zipper strand exchange. Therefore, we conclude that the pH-responsiveness of dynamic properties, both strand exchange time of leucine zipper and stress relaxation time of $AC_{10}A$ networks, are regulated by electrostatic repulsion among negatively charged glutamic acid residues on the *e* and *g* positions in the leucine zipper domain.

3.5. Effects of buffer and salt concentrations on relaxation behavior of $AC_{10}A$ hydrogels

Rheological oscillatory shear measurements of $AC_{10}A$ hydrogels at different buffer and salt concentrations reveal that stress relaxation of these networks becomes slower at higher ionic strength (Figure 3.8 and 3.9). Electrostatic repulsion is screened at high ionic strength, leading to slow strand exchange and network relaxation. Ionic

strength dependence of dynamic properties confirms that they are regulated by electrostatic repulsion.

These rheological data also demonstrate that the control of the structure (hence the plateau storage modulus) and the dynamics (hence the stress relaxation time) of a network can be decoupled (Figure 3.8). The effect of ionic strength on the network topology is imparted through the midblock: the random coil shrinks with increasing ionic strength, which decreases the probability of bridged configurations and reduces the plateau storage modulus. The effect of ionic strength on the dynamics is imparted through the leucine zipper domain: aggregates are stabilized with increasing ionic strength, which leads to a longer stress relaxation time.

4. Conclusions

A strong correlation between the longest stress relaxation time of $AC_{10}A$ hydrogels (τ_r) and the strand exchange time of the leucine zipper domain (τ_2) was found. Both τ_r and τ_2 change significantly in response to pH between 7.0 and 8.0. They are on the same order of magnitude at each pH value and vary with pH in parallel. The molecular basis of the pH-responsiveness of the dynamic properties was the electrostatic repulsion among negatively charged glutamic acid residues on the *e* and *g* positions of the leucine zipper domain. The role of electrostatic repulsion also explains the effect of ionic strength on network relaxation dynamics (τ_r increases with salt concentration).

5. References

(1) Bland, D. R. D. R. *The theory of linear viscoelasticity*; Pergamon Press: Oxford, New York, 1960.

(2) Green, M. S.; Tobolsky, A. V. *Journal of Chemical Physics* **1946**, *14*, 80-92.

(3) Annable, T.; Buscall, R.; Ettelaie, R.; Whittlestone, D. *Journal of Rheology* **1993**, *37*, 695-726.

(4) Jenkins, R. D.; Ph.D. Dissertation; Lehigh University, 1990.

(5) Tanaka, F.; Edwards, S. F. *Journal of Non-Newtonian Fluid Mechanics* **1992**, *43*, 247-271.

(6) Petit-Agnely, F.; Iliopoulos, I. *Journal of Physical Chemistry B* **1999**, *103*, 4803-4808.

(7) Ng, W. K.; Tam, K. C.; Jenkins, R. D. *Journal of Rheology* **2000**, *44*, 137-147.

(8) Petka, W. A.; Ph.D. Dissertation; University of Massachusetts Amherst: Amherst, MA 1997.

(9) Kennedy, S. B.; Ph.D. Dissertation; University of Massachusetts Amherst: Amherst, MA 2001.

(10) Ferry, J. D. *Viscoelastic properties of polymers*; Wiley: New York, 1980.

(11) Macosko, C. W. *Rheology: principles, measurements, and applications*; VCH Publishers, Inc.: New York, N.Y., 1993.

(12) Wendt, H.; Berger, C.; Baici, A.; Thomas, R. M.; Bosshard, H. R. *Biochemistry* **1995**, *34*, 4097-4107.

(13) Urry, D. W. *Journal of Physical Chemistry B* **1997**, *101*, 11007-11028.

Scheme 3.1. Amino acid sequences of proteins discussed in Chapter III.

AC_{10}Atrp (AC_{10}A):
MRGSHHHHHHGSDDDDKASGDLENEVAQLEREVRSLEDEAAELEQKVSRLKNEIEDLKAEIGDHVAPRDTS
YRDPMG[AGAGAGPEG]$_{10}$ARMPTSGDLENEVAQLEREVRSLEDEAAELEQKVSRLKNEIEDLKAEIGDHVAP
RDTSW

Acys:
MRGSHHHHHHGSDDDDKWASGDLENEVAQLEREVRSLEDEAAELEQKVSRLKNEIEDLKAEIGDHVAPRDT
SMGGC

Atrp:
MRGSHHHHHHGSDDDDKASYRDGDLENEVAQLEREVRSLEDEAAELEQKVSRLKNEIEDLKAEIGDPRMPT
SW

TAcys:
MRGSHHHHHHGSDDDDKWASLVPRGSTSGDLENEVAQLEREVRSLEDEAAELEQKVSRLKNEIEDLKAEIG
DHVAPRDTSMGGC

TAtrp:
MRGSHHHHHHGSDDDDKASLVPRGSTSYRDGDLENEVAQLEREVRSLEDEAAELEQKVSRLKNEIEDLKAE
IGDPRMPTSW

Abbreviation for domains:
A: S(D)GDLENEVAQLEREVRSLEDEAAELEQKVSRLKNEIEDLKAE
C_{10}: [AGAGAGPEG]$_{10}$
T: LVPRGS
His-tag: HHHHHH

Table 3.1. Fast and slow characteristic times revealed from strand exchange experiments at different pH

pH	τ_1 (s)	τ_2 (s) (leucine zipper strand exchange time)
7.0	11.7 ± 0.1	4539 ± 121
7.2	16.3± 0.1	2745 ± 28
7.4	17.7 ± 0.2	951 ± 5
7.6	18.7 ± 0.3	496 ± 6
8.0	20.2 ± 0.5	237 ± 4

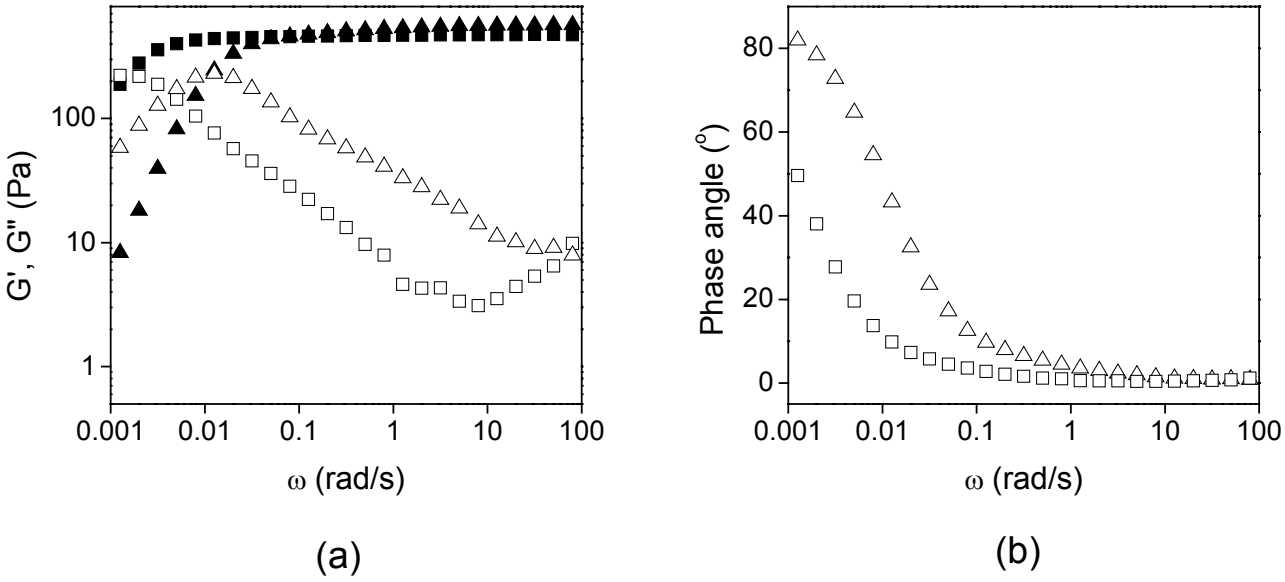

Figure 3.1. Dynamic moduli (G′ closed symbols; G″ open symbols) (a) and phase angle (b) of $AC_{10}A$ hydrogels at pH 7.0 and 8.0. (7% w/v, 100 mM phosphate buffer, 22 ºC) ▲ △ pH 8.0; ■ □ pH 7.0.

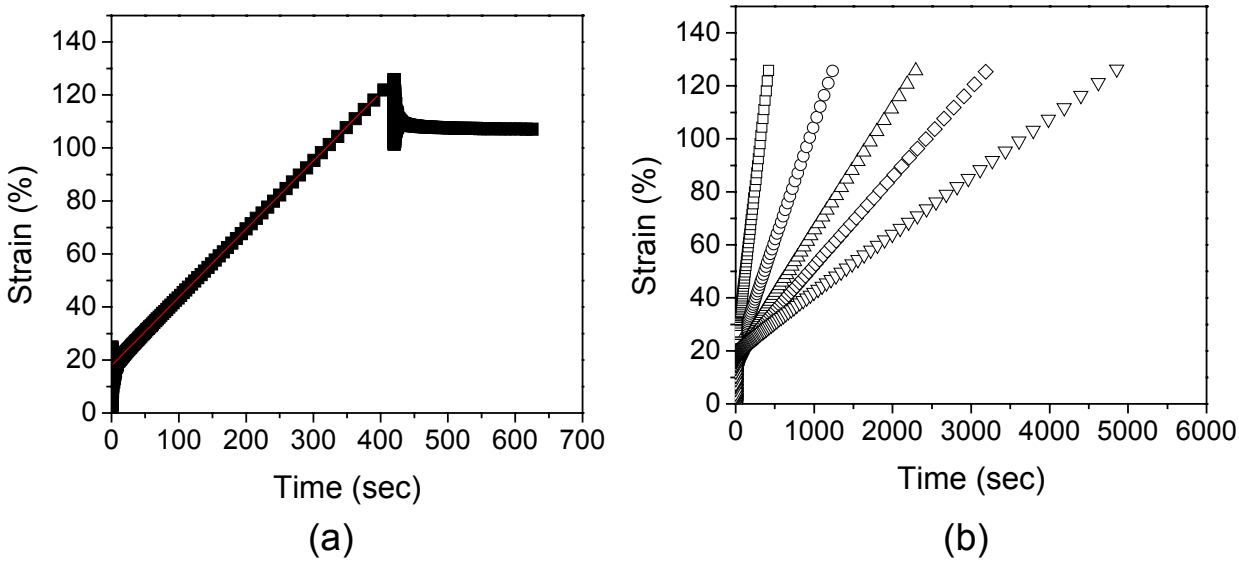

Figure 3.2. Creep measurements for $AC_{10}A$ hydrogels. (a) A creep test for an $AC_{10}A$ hydrogel at pH 8.0. A stress of 100 Pa was applied and removed after 400 seconds. (b) Creep curves of $AC_{10}A$ hydrogels at different pH. Steady rate of straining was confirmed for each test. □ pH 8.0; ○ pH 7.6; △ pH 7.4; ◇ pH 7.2; ▽ pH 7.0. (100 mM phosphate buffer, 7% w/v, T=22 °C, stress=100 Pa)

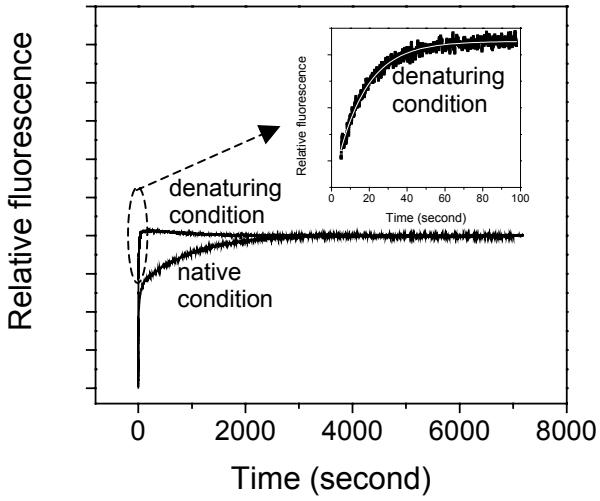

Figure 3.3. Time courses of the increase in fluorescence emission intensity following the mixing of labeled and unlabeled leucine zipper solutions under native condition (in 100 mM phosphate buffer) and denaturing condition (in 8 M urea). (100 μM leucine zipper solutions, pH 7.4, 22 °C)

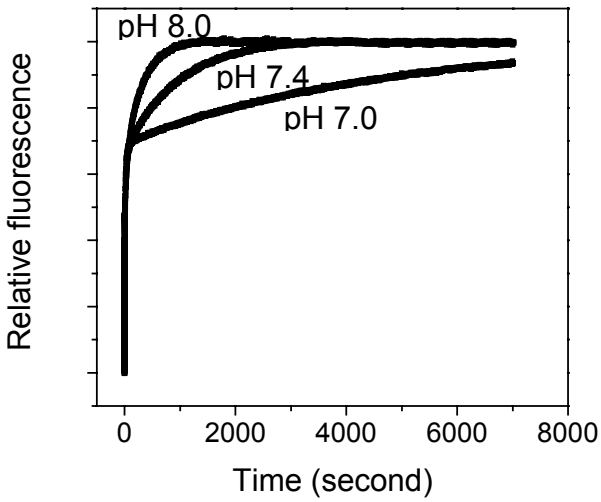

Figure 3.4. Time courses of the increase in fluorescence emission intensity following the mixing of labeled and unlabeled leucine zipper solutions at different pH. (100 μM leucine zipper A, 100 mM phosphate buffer, 22 °C)

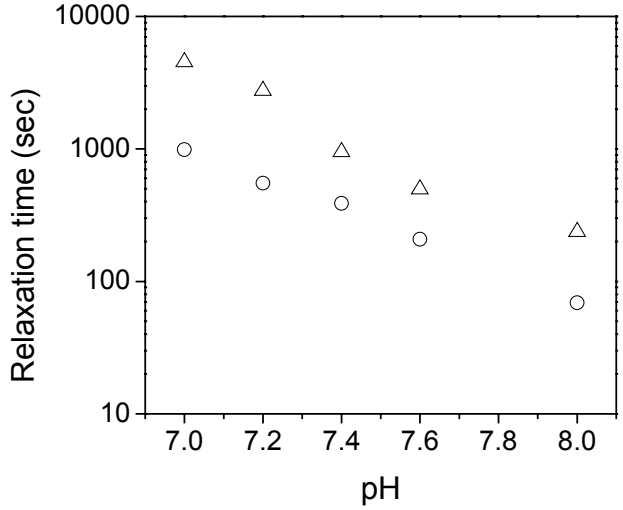

Figure 3.5. Correlation between the longest stress relaxation time of $AC_{10}A$ hydrogels (7% w/v) (○) and the strand exchange time of leucine zipper A (in 100 μM solutions) (△). (100 mM phosphate buffer, 22 °C)

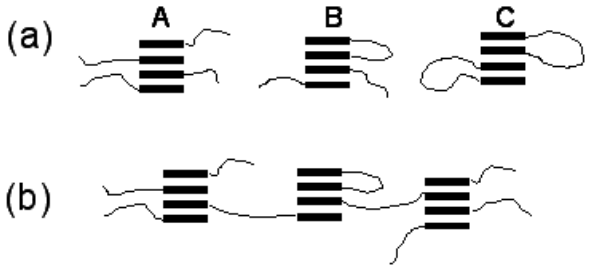

Figure 3.6. (a) Three possible states for tetrameric leucine zipper aggregates in a network. The functionalities for A, B, and C are 4, 2, and 0, respectively. (b) A superbridge.

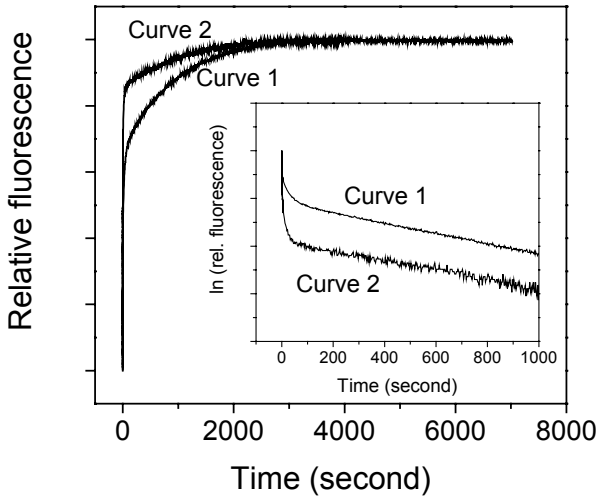

Figure 3.7. Removal of the histidine tag does not affect leucine zipper strand exchange kinetics. Exponential decay fitting revealed that the strand exchange times are 950.9 ± 5.1 seconds (curve 1, Acys-FM + Atrp) and 955.6 ± 13.0 seconds (curve 2, no-6H-TAcys-FM + no-6H-TAtrp), respectively, before and after removing the histidine tag. (100 mM phosphate buffer, 100 μM leucine zipper, pH 7.4, 22 °C)

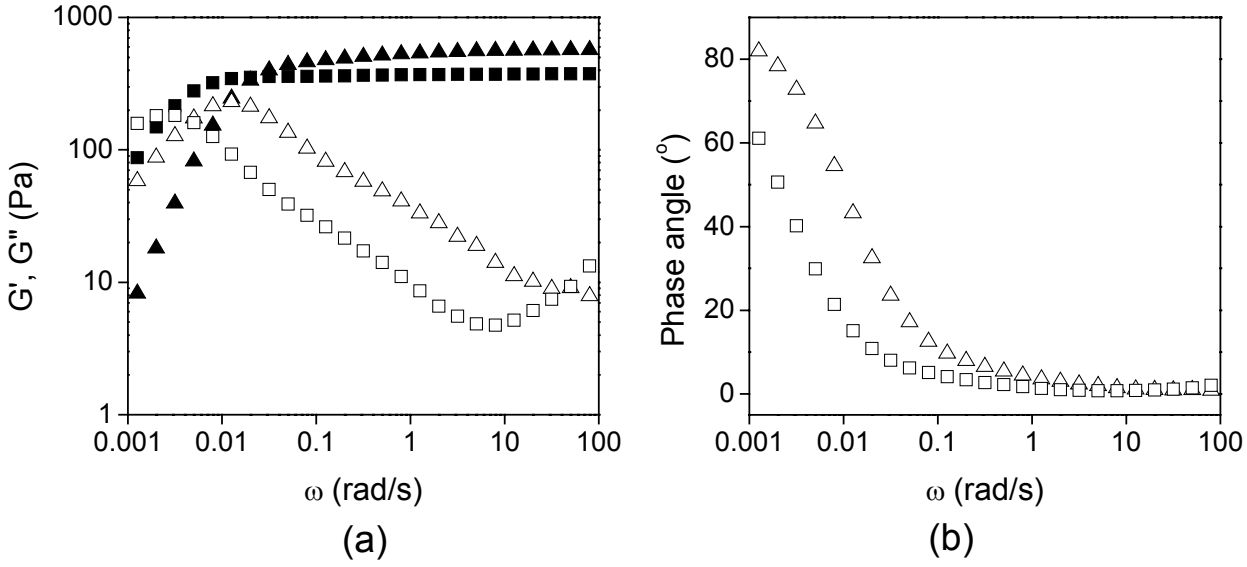

Figure 3.8. Effect of NaCl concentration on dynamic moduli (G′ closed symbols; G″ open symbols) (a) and phase angle (b) of $AC_{10}A$ hydrogels at pH 8.0. (7% w/v, 100 mM phosphate buffer, 22 ºC) ▲ △ No NaCl; ■ □ 400 mM NaCl.

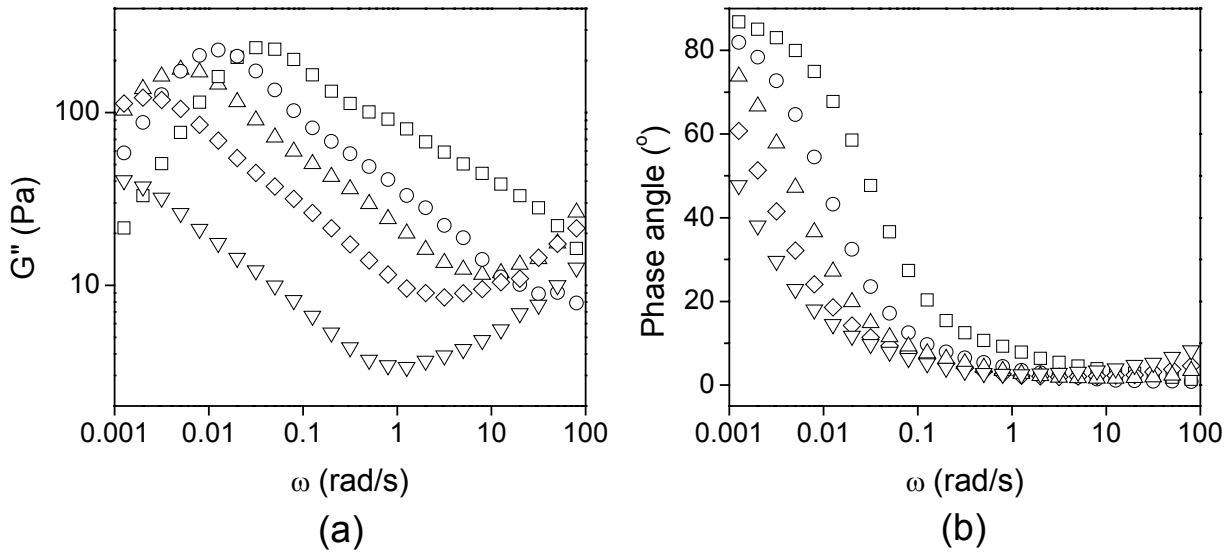

Figure 3.9. Effect of phosphate buffer concentration on loss moduli (a) and phase angles (b) of $AC_{10}A$ hydrogels at pH 8.0. (7% w/v, 22 ºC) □ 10 mM; ○ 100 mM; △ 200 mM; ◇ 300 mM; ▽ 400 mM.